

Electronic Supplementary Information

A homologous series of macrocyclic Ni clusters: Synthesis, structures, and catalytic properties

Huixin Xiang,^{a,b, ‡} Ranran Cheng,^{b, ‡} Chenhao Ruan,^{a,b} Changqing Meng,^{a,b} Yuzheng Gan,^{a,b} Wanyu Cheng,^a Yue Zhao,^c Cong-Qiao Xu,^{* d} Jun Li,^{d,e} and Chuanhao Yao^{* a,b}

^a Strait Institute of Flexible Electronics, Fujian Normal University, Fuzhou 350117, China

E-mail: ifechhyao@fjnu.edu.cn

^b Institute of Flexible Electronics (IFE), Northwestern Polytechnical University, Xi'an 710072, China

^c Coordination Chemistry Institute, State Key Laboratory of Coordination Chemistry, School of Chemistry and Chemical Engineering, Nanjing University, Nanjing 210023, China

^d Department of Chemistry, Southern University of Science and Technology, Shenzhen 518055, China. E-mail: xucq@sustech.edu.cn

^e Department of Chemistry and Engineering Research Center of Advanced Rare-Earth Materials of Ministry of Education, Tsinghua University, Beijing 10084, China

[‡]Equal contribution: Huixin Xiang and Ranran Cheng

Table of Contents

1. Materials	S3
2. Synthesis	S3
3. Purification and Crystallization of the nickel clusters homologues.....	S3
4. Stability tests.....	S4
5. Catalytic reduction of 4-Nitrophenol	S4
6. Characterizations.....	S4
7. Computational methods	S5
References.....	S5
8. Supporting figures.....	S6
Fig. S1	S6
Fig. S2.....	S7
Fig. S3	S8
Fig. S4.....	S9
Fig. S5.....	S10
Fig. S6.....	S11
Fig. S7.....	S12
Fig. S8.....	S13
Fig. S9.....	S14
Fig. S10.....	S15
Fig. S11	S16
Fig. S12.....	S17
Fig. S13.....	S18
Table S1.	S19

1. Materials

The water used in all experiments was ultrapure (resistivity 18.2 M Ω cm), produced with a PURELAB pure water system. The following chemicals and solvents were purchased from various sources and used as received without further purification. Nickel (II) chloride hexahydrate (NiCl₂·6H₂O, 99%), 4-methylphenthiofenol (4MPT, 98%), tetrahydrofuran (THF, 99.8%), acetic acid (CH₃COOH, 99%), and p-Nitrophenol (99%) were received from Adamas. Methanol (99.8%), ethanol (99.8%), dichloromethane (DCM, 99.9%), and potassium hydroxide (KOH, 90%) were received from Greagent. Sodium borohydride (NaBH₄, 99.99%), toluene (99.8%), and hydrogen peroxide (H₂O₂, 30%) were purchased from Sinopharm Chemical Reagent Co., Ltd.

2. Synthesis

The clusters were synthesized by a one-pot method. Typically, in a 50 mL round-bottom flask, 24 mg of NiCl₂·6H₂O was dissolved in 20 mL ethanol and then stirred under vigorous stirring to dissolve the nickel chloride hexahydrate rapidly. The color of the solution changed from colorless to green. After 15 minutes, 15 mg of 4MPT was added, and the solution was stirred for 30 minutes. Then, 13.7 mg of NaBH₄ (in 3 mL ethanol) was quickly added, and the color of the solution quickly changed from green to dark. The reaction lasted for 12 hours at room temperature.

3. Purification and Crystallization of the nickel clusters homologues

After reaction, the crude products were collected by centrifugation and washed with ethanol for three times. Subsequently, 2 mL of CH₂Cl₂ was used to extract the nickel clusters homologues from the crude cluster product. To separate the nickel clusters homologues, thin-layer chromatography (TLC) was employed. A mixture of CH₂Cl₂ and petroleum ether was used as the developing solvent with a volume ratio as 1:3. The yield of Ni₉(4MPT)₁₈, Ni₁₀(4MPT)₂₀, Ni₁₁(4MPT)₂₂, and Ni₁₂(4MPT)₂₄ clusters are ~7%, 10%, 8%, and 5%, respectively. The crystals of Ni₉(4MPT)₁₈, Ni₁₀(4MPT)₂₀, Ni₁₁(4MPT)₂₂, and Ni₁₂(4MPT)₂₄ clusters were achieved after one week by diffusing methanol into a toluene solution of the clusters.

4. Stability tests

The chemical stability tests of the clusters were conducted by adding different reagents (including CH₃COOH, KOH, and NaBH₄) to a toluene solution of each cluster and time dependent UV-vis-NIR spectrometry was adopted to monitor the spectra change of each cluster. Specifically, 0.5 mg of each cluster was dissolved in 2 mL THF, and an initial UV-vis-NIR spectrum was recorded. Subsequently, 30 μ L 1M acetic acid solution was added to the solution of the cluster, and another UV-vis-NIR spectrum was recorded. Next, for each round of acetic acid addition (30 μ L), a spectrum was recorded. Stability tests under alkaline, or reducing environments were proceeded in a similar way as aforementioned, except that KOH (30 μ L, 1M), or NaBH₄ (15 mg), respectively, instead of acetic acid was employed in the reaction. For thermal stability tests of the clusters, time dependent UV-vis-NIR spectra were recorded for each cluster which was dissolved in toluene at 60 °C.

5. Catalytic reduction of 4-Nitrophenol

The catalytic reduction of 4-Nitrophenol was carried out in a 4 mL quartz cuvette. 30 μ L 4-Nitrophenol solution (20 mM) was added to 2.5 mL tetrahydrofuran. Then 0.01 μ mol of each cluster was added to the above solution, followed by 0.5 mL freshly prepared NaBH₄ solution (0.48 M). The cuvette was then placed in the sample holder of the UV-vis spectrometer. The progress of the reaction was tracked by monitoring the changes of the absorbance intensity of 4-Nitrophenol at 400 nm as a function of time.

6. Characterizations

ESI-MS data of the clusters was recorded on an Agilent Technologies ESI-TOF-MS spectrometer and cesium acetate was added to charge the cluster. Single crystal X-ray diffraction data was collected on a Bruker APEX II CCD diffractometer, using graphite-monochromated and 0.5 mm MonoCap collimated Mo-K α radiation ($\lambda = 0.71073 \text{ \AA}$) with the ω scan method. Data were processed with the INTEGRATE program of the APEX2 software for reduction and cell refinement. The UV/vis/NIR absorption spectra were measured on a P9 Dual Beam UV-Visible Spectrophotometer (Mapada, Shanghai)

at room temperature.

7. Computational methods

To investigate the electronic structures of nickel clusters, quantum chemical calculations based on density functional theory were performed using Amsterdam Density Functional (ADF 2019.304) program.^{1,2} The zero-order-regular approximation (ZORA)³ was applied to estimate the scalar relativistic effects. Geometry optimizations were carried out with Perdew-Burke-Ernzerh (PBE) exchange-correlation functional,⁴ together with DZ basis sets. To simulate the UV-Vis spectra and interpret the optical properties, density of states and time-dependent DFT (TDDFT) calculations were performed based on the optimized structures using the LB94 potential,⁵ with DZ basis sets applied for Ni, S atoms and SZ used for C, H atoms, respectively. Frozen core approximations were utilized to the inner shells $[1s^2-2p^6]$ for Ni, $[1s^2]$ for S and $[1s^2]$ for C atom. The lowest 1500, 2000, 3000 and 1800 excited states were considered for the TDDFT calculations of $Ni_9(4MPT)_{18}$, $Ni_{10}(4MPT)_{20}$, $Ni_{11}(4MPT)_{22}$ and $Ni_{12}(4MPT)_{24}$ clusters, respectively.

References:

(1) te Velde, G.; Bickelhaupt, F. M.; Baerends, E. J.; Fonseca Guerra, C.; van Gisbergen, S. J. A.; Snijders, J. G.; Ziegler, T. Chemistry with ADF. *J. Comput. Chem.* **2001**, *22*, 931-967.

(2) Fonseca Guerra, C.; Snijders, J. G.; te Velde, G.; Baerends, E. J. Towards an order-N DFT Method. *Theor. Chem. Acc.* **1998**, *99*, 391-403.

(3) van Lenthe, E.; Baerends, E. J.; Snijders, J. G. Relativistic Regular Two-Component Hamiltonians. *J. Chem. Phys.* **1993**, *99*, 4597-4610.

(4) Perdew, J. P.; Burke, K.; Ernzerhof, M. Generalized Gradient Approximation Made Simple. *Phys. Rev. Lett.* **1996**, *77*, 3865-3868.

(5) van Leeuwen, R.; Baerends, E. J. Exchange-Correlation Potential with Correct Asymptotic Behavior. *Phys. Rev. A* **1994**, *49*, 2421-2431.

8. Supporting figures

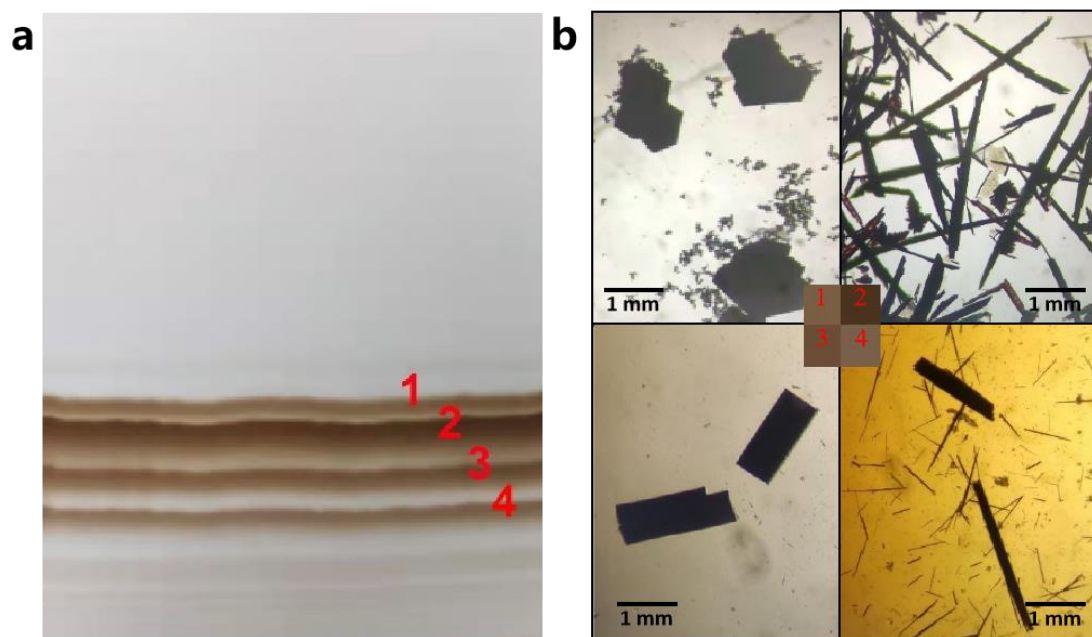


Fig. S1 (a) Photograph of the $\text{Ni}_n(4\text{MPT})_{2n}$, ($n=9-12$) clusters separated by TLC. (b) The single crystal morphology of the clusters. Number 1 to 4 correspond to $\text{Ni}_9(4\text{MPT})_{18}$, $\text{Ni}_{10}(4\text{MPT})_{20}$, $\text{Ni}_{11}(4\text{MPT})_{22}$, and $\text{Ni}_{12}(4\text{MPT})_{24}$, respectively.

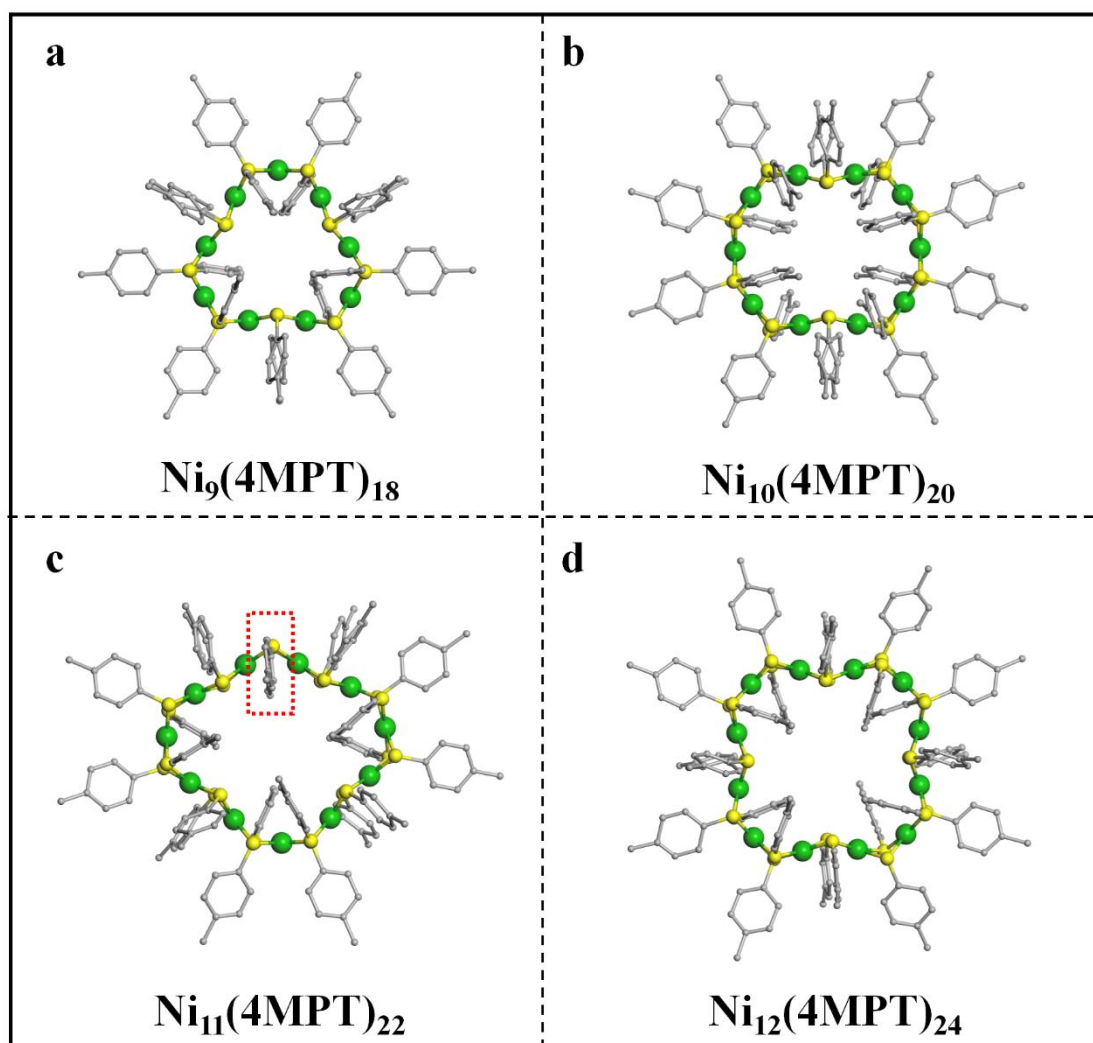


Fig. S2 Top view of the molecular structures of (a) $\text{Ni}_9(4\text{MPT})_{18}$, (b) $\text{Ni}_{10}(4\text{MPT})_{20}$, (c) $\text{Ni}_{11}(4\text{MPT})_{22}$ and (d) $\text{Ni}_{12}(4\text{MPT})_{24}$. Color codes: green, Ni; yellow, S; gray, C. All H atoms are omitted for clarity. Note, the red dashed box in Fig. S2c highlights the two axial substituents bent inward the $\text{Ni}_{11}\text{S}_{22}$ ring.

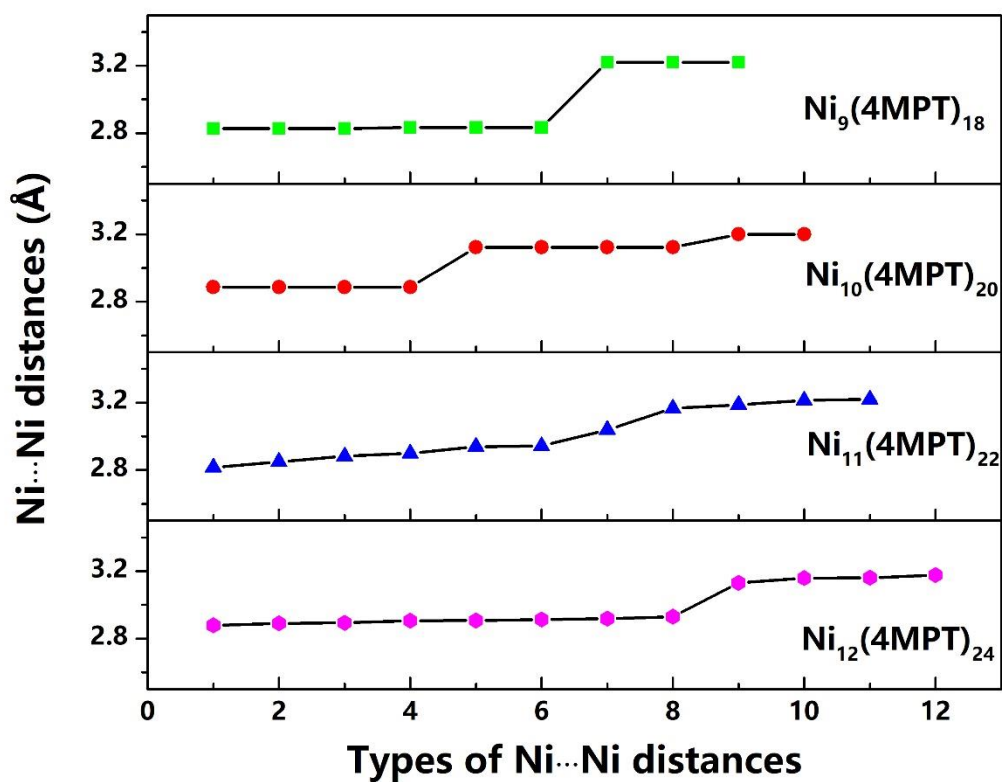


Fig. S3 The Ni...Ni distances in Ni_nS_{2n} frameworks of the Ni_n(4MPT)_{2n} clusters.

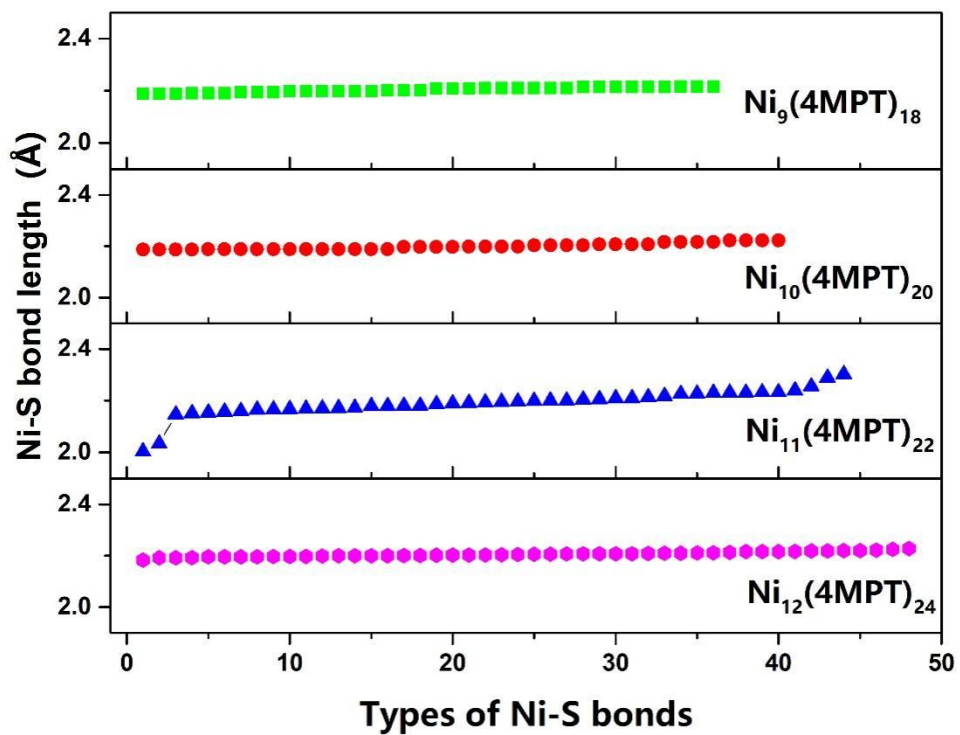


Fig. S4 Ni-S bond lengths in Ni_nS_{2n} frameworks of the Ni_n(4MPT)_{2n} clusters.

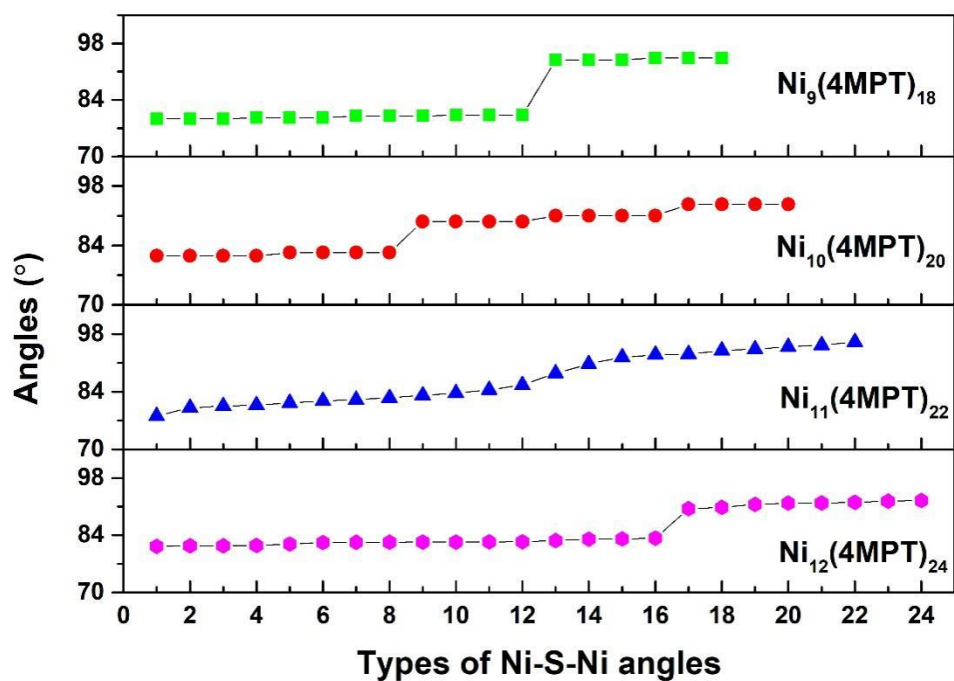


Fig. S5 The Ni-S-Ni angles in Ni_nS_{2n} frameworks of the Ni_n(4MPT)_{2n} clusters.

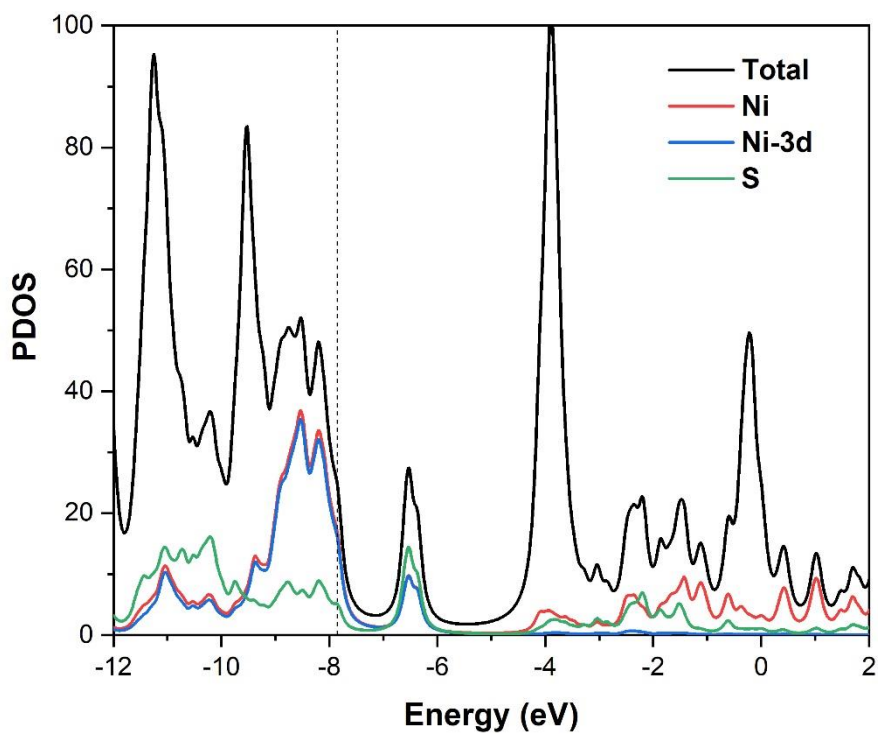


Fig. S6 Projected density of states (PDOS) of Ni₁₂(4MPT)₂₄ cluster with the LB94 functional and a Lorentzian width of 0.10 eV, where the dashed line corresponds to the Fermi level (HOMO).

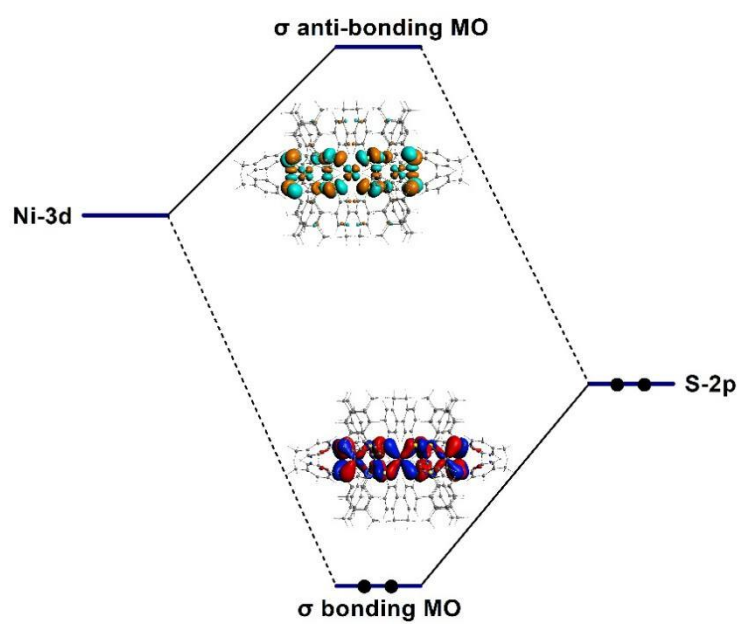


Fig. S7 Schematic orbital interaction diagram between Ni-3d and S-2p orbitals that contribute to the vacant σ anti-bonding MOs of Ni clusters (isovalue = 0.015 a.u.).

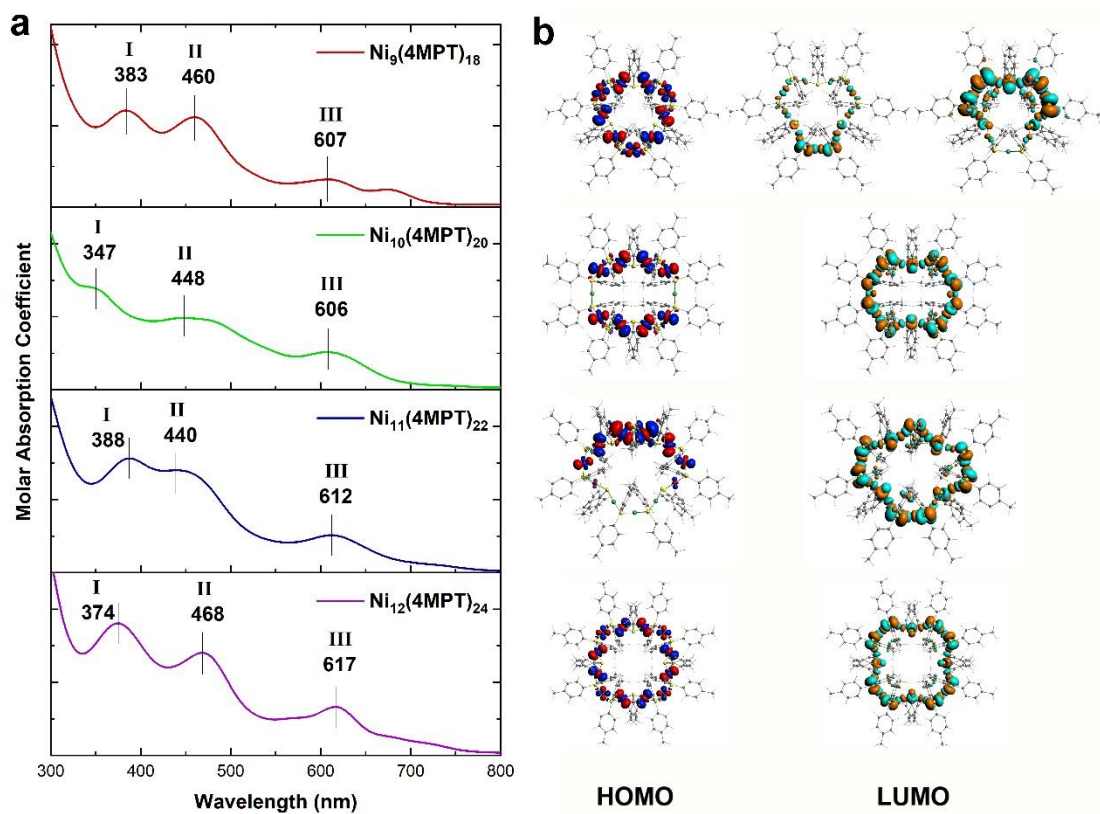


Fig. S8 (a) The simulated UV-Vis-NIR spectra of the nickel clusters at the TDDFT/LB94 SR-ZORA level of theory, with the Gaussian half-width of 45 nm. (b) The HOMO and LUMO of Ni clusters using the PBE functional (isovalue = 0.015 a.u.).

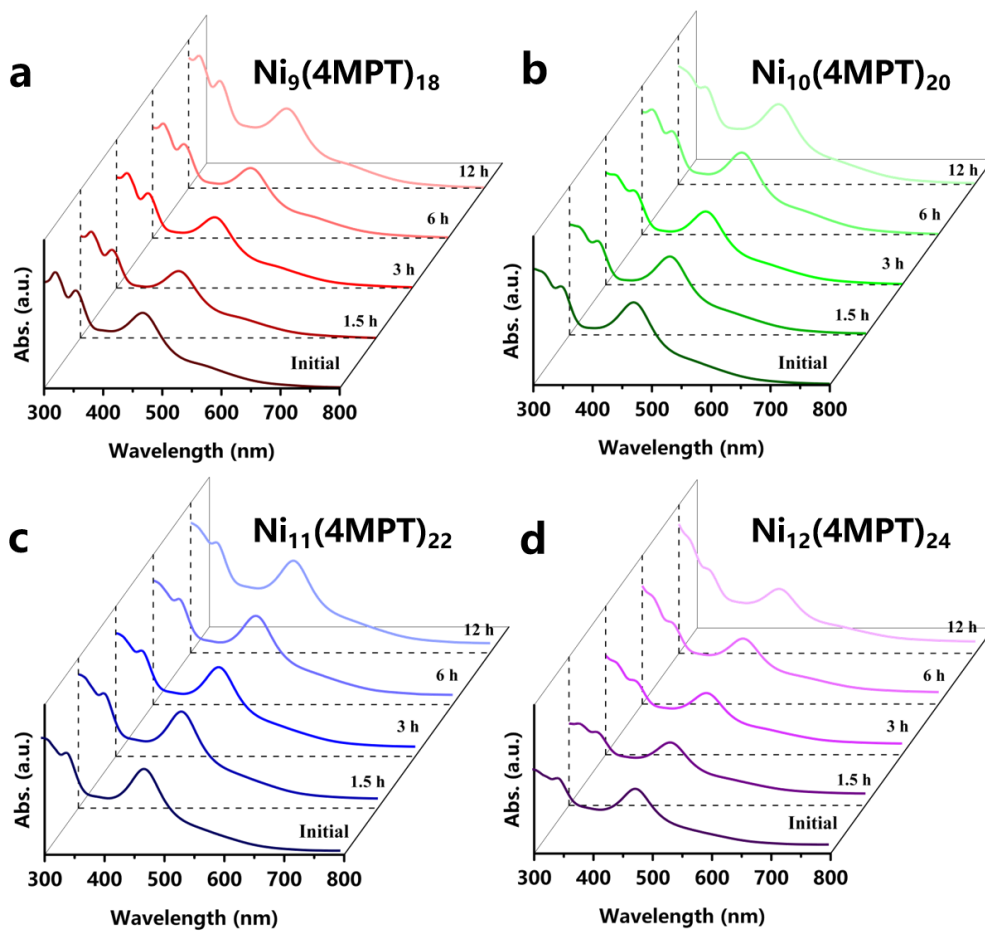


Fig. S9 Thermal stability tests of the $\text{Ni}_n(4\text{MPT})_{2n}$ clusters. Time-dependent UV-vis-NIR spectra show the stability of (a) $\text{Ni}_9(4\text{MPT})_{18}$, (b) $\text{Ni}_{10}(4\text{MPT})_{20}$, (c) $\text{Ni}_{11}(4\text{MPT})_{22}$, and (d) $\text{Ni}_{12}(4\text{MPT})_{24}$ at 60 °C in toluene solution.

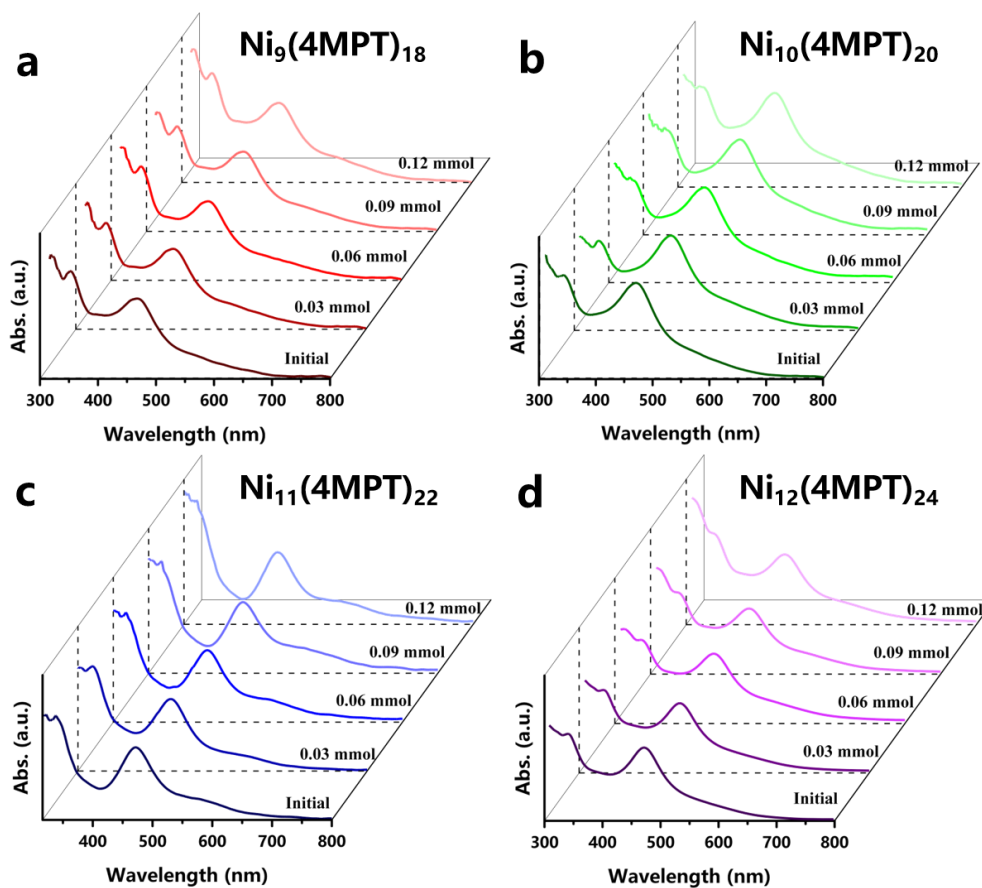


Fig. S10 Acid resistance tests of the clusters. UV-vis-NIR spectra recorded after the addition of different amounts of CH₃COOH into the solutions of the clusters. (a) Ni₉(4MPT)₁₈, (b) Ni₁₀(4MPT)₂₀, (c) Ni₁₁(4MPT)₂₂, and (d) Ni₁₂(4MPT)₂₄.

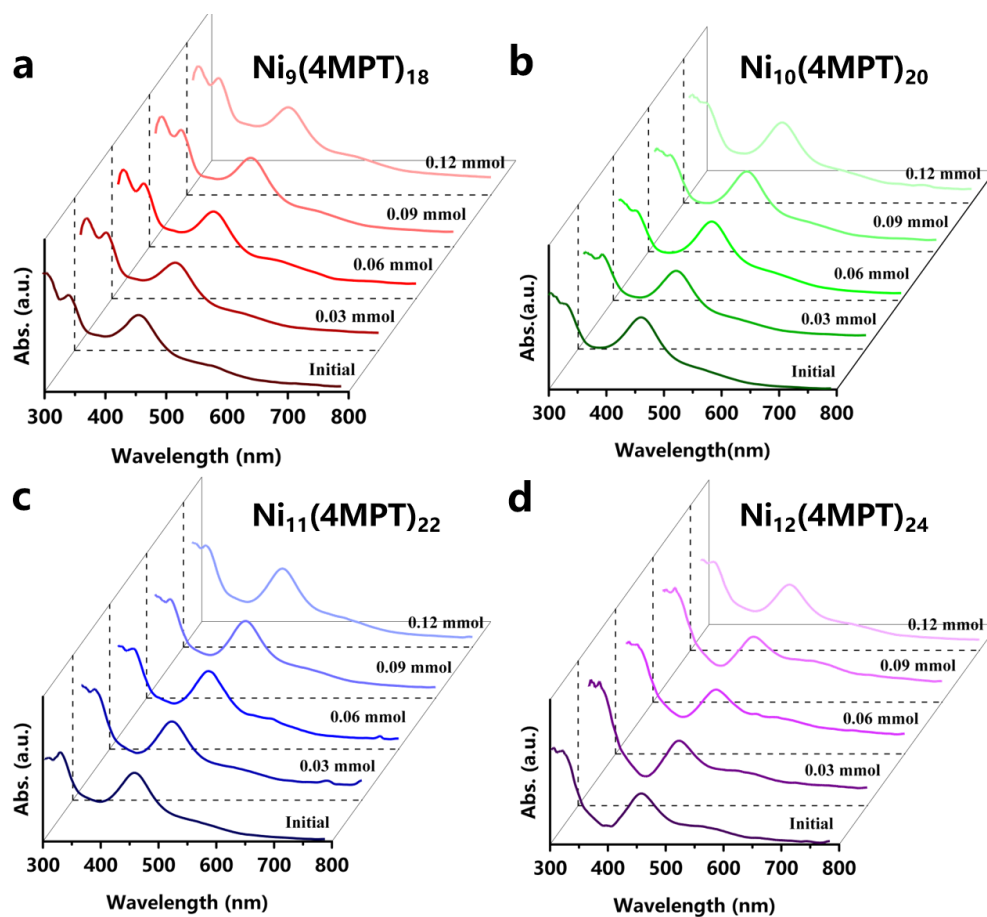


Fig. S11 Alkalinity resistance tests of the clusters. UV-vis-NIR spectra recorded after the addition of different amounts of KOH into the solutions of the clusters, (a) $\text{Ni}_9(4\text{MPT})_{18}$, (b) $\text{Ni}_{10}(4\text{MPT})_{20}$, (c) $\text{Ni}_{11}(4\text{MPT})_{22}$, and (d) $\text{Ni}_{12}(4\text{MPT})_{24}$.

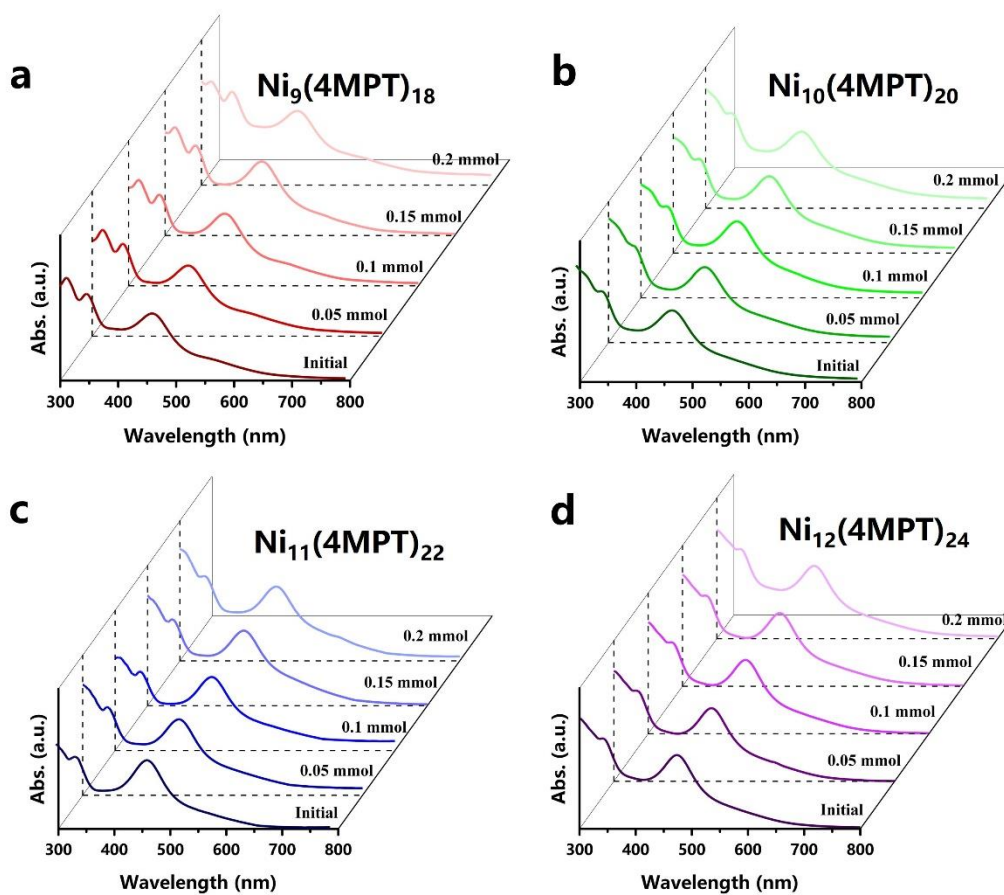


Fig. S12 The stability tests of the clusters in reducing condition. UV-vis-NIR spectra recorded after the addition of different amounts of NaNH_4 into the solutions of the clusters, (a) $\text{Ni}_9(4\text{MPT})_{18}$, (b) $\text{Ni}_{10}(4\text{MPT})_{20}$, (c) $\text{Ni}_{11}(4\text{MPT})_{22}$, and (d) $\text{Ni}_{12}(4\text{MPT})_{24}$.

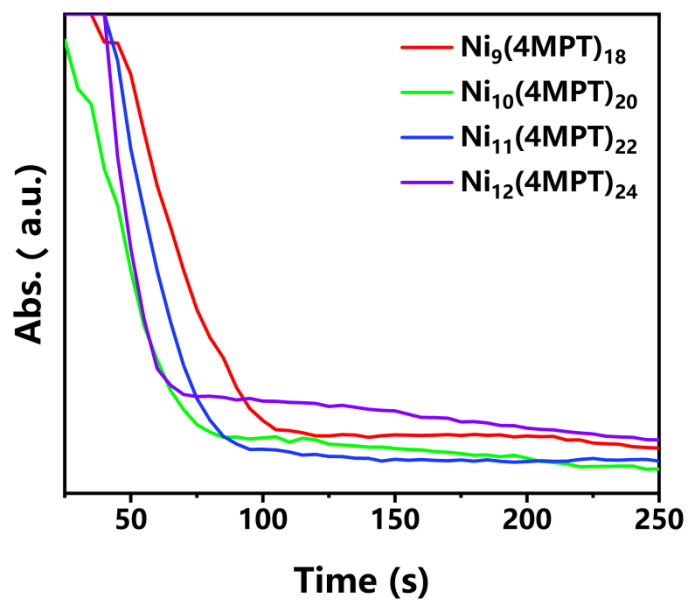


Fig. S13 Time-dependent UV-vis absorption at 400 nm in the reduction reaction of p-nitrophenol catalyzed by $\text{Ni}_n(4\text{MPT})_{2n}$ clusters.

Table S1. Point group symmetries, average bond lengths (in parentheses are the experimental values) and the corresponding Mayer bond orders for the optimized structures of Ni clusters at the PBE/DZ SR-ZORA level of theory.

Cluster	Symmetry	Bond length (Å)			Bond order		
		Ni-Ni ^a	Ni-Ni ^b	Ni-S	Ni-Ni ^a	Ni-Ni ^b	Ni-S
Ni ₉ (4MPT) ₁₈	<i>D</i> ₃	2.86(2.83)	3.30(3.22)	2.28(2.20)	0.21	0.07	0.71
Ni ₁₀ (4MPT) ₂₀	<i>D</i> ₂	2.90(2.89) 3.16(3.12)	3.27(3.20)	2.27(2.20)	0.19 0.10	0.08	0.72
Ni ₁₁ (4MPT) ₂₂	<i>C</i> ₁	2.93(2.91) 3.28(3.20)	2.84(2.90)	2.27(2.19)	0.18 0.08	0.22	0.71
Ni ₁₂ (4MPT) ₂₄	<i>D</i> ₄	2.96(2.91)	3.25(3.16)	2.27(2.21)	0.17	0.10	0.71

^a The Ni-Ni bond lengths inside the equivalent units shown in Fig. 1.

^b The Ni-Ni bond lengths between the equivalent units shown in Fig. 1.